Constrained Deep Learning-based Model Predictive Control with Improved Constraint Satisfaction

Farshid Asadi and Jingang Yi

***Abstract*— Machine learning technique can help reduce computational cost of model predictive control (MPC). In this paper, a constrained deep neural networks design is proposed to learn and construct MPC policies for nonlinear input affine dynamic systems. Using constrained training of neural networks helps enforce MPC constraints effectively. We show the asymptotic stability of the learned policies. Additionally, different data sampling strategies are compared in terms of their generalization errors on the learned policy. Furthermore, probabilistic feasibility and optimality guarantees are provided for the learned control policy. The proposed algorithm is implemented on a rotary inverted pendulum experimentally and control performance is demonstrated and compared with the exact MPC and the normally trained learning MPC. The results show that the proposed algorithm improves constraint satisfaction while preserves computational efficiency of the learned policy.**

I. Introduction

Model predictive control (MPC) is an advanced control technique based on optimization while considering system constraints [1]. One challenge of widely application of MPC is the high computational demand of the corresponding optimization problem [2]. Over the past two decades, various approaches are proposed to solve the scalability challenge. Fast solvers tailored to the structure of the MPC optimization are used in [2] and implemented on embedded systems (e.g., [3]). Soft constraint formulation of hard constraints is proposed to relax hard constraints and alleviate computational cost of MPC [4]. However, they are not widely used because of non-strict nature of constraint satisfaction. Explicit MPC (EMPC) technique for linear systems is another approach for reducing computational burden. The main idea of EMPC is to pre-compute the control laws offline and use them in online operation [5]. However, computational demand and memory requirement in EMPC rise dramatically as the size of the problem increases [6]. A plausible solution to alleviate this, is to use various approximated EMPC methods. Recent advances in machine learning techniques, such as deep neural networks (DNNs), bring new opportunities to integrate with EMPC [7]. For example, piece-wise affine property of solution to linear MPC is used to show the learnability of linear MPC policies [8]–[12]. Deep EMPC for nonlinear systems is proposed in [13]–[15]. Optimality and constraint satisfaction of the learned policy is an important concern. In [10], [13], [15], probabilistic confidence level for feasibility is proposed based on post validation [16]. The work in [11], [12] use neural network structure properties to guarantee control design feasibility but limited to linear time invariant systems. Furthermore, no explicit method is introduced for imposing constraints on DNN.

To improve constraint satisfaction for deep learning-based EMPC, we consider to enforce constraints during training process. Up until recently, DNNs output constraints are usually modeled as soft constraints [17], namely, adding constraints as a penalty to loss function. It is not straightforward to choose weighting factors and constraint satisfaction is not guaranteed [17]. It is possible to include hard constraints in training DNNs. For example, equality output constraints of DNNs are considered and the method of Lagrange multiplier is used in [17]. The other approach in [18] covers inequality constraints and a constrained training problem is solved by applying alternating stochastic gradient descent/ascent iteratively.

For many deep EMPC algorithms (e.g., [10], [13], [15]), no constraint is enforced during training stage. Some algorithms use relatively computationally heavy methods to enforce constraints in training [9], and others only enforce simple bound constraints on the neural network [8]. In this work, we use constrained DNN to learn MPC policies for nonlinear systems while enforcing constraints during training. Lagrange multipliers are used to directly incorporate constraints in DNN training. All inequality constraints are rewritten into equality constraints and it leads to overcome myriad number of constraints in the sampled problem. After that, we convert the constrained optimization problem in DNN training to an unconstrained max-min optimization. Finally, a two-step alternating approach is used to solve the resulted max-min optimization. Comparing with the existing methods of deep learning-based MPC (e.g., [8], [10], [13], [15]), the proposed approach explicitly enforces constraints during training process. Unlike the method in [9], the improved constraint satisfaction is achieved without adding extra computational burden in the final learned policy. We also provide stability analysis for the learned policy. Furthermore, we performed an analysis of data sampling techniques based on their generalization errors of the learned policies. The proposed constrained deep EMPC algorithm is implemented on an underactuated rotary pendulum and its performance is compared with the exact MPC method and the normally trained deep EMPC. The main contribution of this work lies in the new deep learning-based EMPC for nonlinear dynamics with improved constraint satisfaction and guaranteed stability.

The remainder of the paper is organized as follows. We present the problem formulation in Section II. The main results are presented in Section III. We present case study and experiments in Section IV. Finally, we summarize the concluding remarks in Section V.

II. Problem Statement and Preliminaries

A. Problem Statement

Consider the following discrete-time nonlinear system

$$\boldsymbol{x}_{k+1} = \boldsymbol{f}(\boldsymbol{x}_k) + \boldsymbol{g}(\boldsymbol{x}_k)\boldsymbol{u}_k, \tag{1}$$

where $\boldsymbol{x} \in \mathbb{R}^{n\times 1}$ is the state variable, $\boldsymbol{u} \in \mathbb{R}^m$ is the control input, $\boldsymbol{f}(\boldsymbol{x}) \in \mathbb{R}^n$ and $\boldsymbol{g}(\boldsymbol{x}) \in \mathbb{R}^{n\times m}$ are system drift and input matrices, respectively. The MPC is formulated for (1) as the following optimization problem [1].

$$V(\boldsymbol{x}_k) = \min_{\boldsymbol{U}_k} \Bigg[\sum_{i=0}^{H-1} \left(\boldsymbol{x}_{i|k}^T \boldsymbol{Q} \boldsymbol{x}_{i|k} + \boldsymbol{u}_{i|k}^T \boldsymbol{R} \boldsymbol{u}_{i|k} \right) + \boldsymbol{x}_{H|k}^T \boldsymbol{Q}_f \boldsymbol{x}_{H|k} \Bigg] \tag{2a}$$

$$\text{s.t. } \boldsymbol{x}_{i+1|k} = \boldsymbol{f}(\boldsymbol{x}_{i|k}) + \boldsymbol{g}(x_{i|k})\boldsymbol{u}_{i|k}, \tag{2b}$$

$$\boldsymbol{C}\left(\boldsymbol{x}_{i|k}, \boldsymbol{u}_{i|k}\right) \leq \boldsymbol{0},\ \boldsymbol{C}_f(\boldsymbol{x}_{H|k}) \leq \boldsymbol{0}, \tag{2c}$$

$$\boldsymbol{x}_{0|k} = \boldsymbol{x}_k, \boldsymbol{u}_{-1|k} = \boldsymbol{u}_{k-1}, i = 0, \ldots, H-1, \tag{2d}$$

where k is a dummy index representing current sampling time (due to time invariant dynamics [19]), i is sampling time over control horizon from the kth step, $\boldsymbol{x}_{i|k}$ and $\boldsymbol{u}_{i|k}$ are the state vector and the control input at the ith step of the control horizon with respect to current step (i.e., k), $i = 0, \ldots, H-1$, H is the control horizon, $\boldsymbol{U}_k = [\boldsymbol{u}_{0|k}^T, \ldots, \boldsymbol{u}_{H-1|k}^T]^T$ is the control sequence set. Matrices $\boldsymbol{Q} \succ 0$, $\boldsymbol{Q}_f \succ 0 \in \mathbb{R}^{n\times n}$ and $\boldsymbol{R} \succ 0 \in \mathbb{R}^{m\times m}$ are positive definite, where operator "$\succ$" stands for positive definite for a matrix and $\boldsymbol{C} \leq \boldsymbol{0}$ in (2c) represents element-wise operation for vector $\boldsymbol{C} \in \mathbb{R}^{n_c}$ that defines constraints on state variable and control input. $\boldsymbol{C}_f \in \mathbb{R}^{n_f}$ also defines terminal set of the system guaranteeing recursive feasibility of the problem, where n_c and n_f are the constraint numbers for total and the terminal constraints, respectively. Furthermore, we assume that all constraint sets are compact sets.

The MPC problem must be solved at each time step k and only first element of control sequence $\boldsymbol{U}_k$ is applied to the system, that is,

$$\boldsymbol{u}_k^* = \boldsymbol{u}_{0|k}^*. \tag{3}$$

The problem statement for this work is given as follows: obtain the control policy in (3) with a DNN while enforcing constraints of (2) during training process. The goal is to obtain a computationally efficient approximate MPC policy with improved constraint satisfaction. In the rest of this section, we introduce some background and preliminaries that are useful in following sections.

B. Preliminaries

DNNs has shown promising potentials in different learning schemes [7]. In this work, deep multilayer perceptron (MLP) is used to approximate the MPC policy with computationally efficient closed form. A deep MLP can be described in the following form [7].

$$\mathcal{N}(\boldsymbol{x}; \boldsymbol{\theta}, M, l) = f_{l+1} \circ g_l \circ f_l \circ \cdots \circ g_1 \circ f_1(\boldsymbol{x}), \tag{4}$$

where $\boldsymbol{x} \in \mathbb{R}^n$ and $\mathcal{N} \in \mathbb{R}^m$ are the neural network input and output, respectively, M is the number of hidden nodes per layer, l is the number of hidden layers, and $\boldsymbol{\theta}$ is the network parameters. $f_i(\cdot)$ is a linear affine map between each layer and $g_i(\cdot)$ is nonlinear activation function, $i = 1, \ldots, l$. The goal in constrained deep learning is to find $\boldsymbol{\theta}$ to minimize loss function while satisfying given constraints on output of the neural network

$$\min_{\boldsymbol{\theta}}\ \mathcal{L}(\boldsymbol{\theta}) = \frac{1}{N} \sum_{i=0}^{N} L\left(\boldsymbol{y}_i - \hat{\boldsymbol{y}}(\boldsymbol{x}_i)\right) \tag{5a}$$

$$\text{s.t. } \boldsymbol{C}(\boldsymbol{\theta}, \hat{\boldsymbol{y}}(\boldsymbol{x}_i)) \leq \boldsymbol{0},\ i = 1, \ldots, N. \tag{5b}$$

where L is mean square error loss function, $\boldsymbol{x}_i$ is the ith sample of $\boldsymbol{x}$, $\boldsymbol{y}_i \in \mathbb{R}^m$ is the vector assigned to $\boldsymbol{x}_i$ by the underlying function, $\hat{\boldsymbol{y}} = \mathcal{N}(\boldsymbol{x}; \boldsymbol{\theta}, M, l)$ is the DNN prediction for $\boldsymbol{y}$, and N is the total sampling number. Inequality in (5) represents element-wise operation for vector $\boldsymbol{C} \in \mathbb{R}^{n_c}$ that defines constraints on output of the neural network.

To analyze empirical guarantees of optimality and constraint satisfaction of (5), we introduce the following indicators for optimality and constraint satisfaction

$$I_o(\boldsymbol{x}) = \begin{cases} 1, \|\boldsymbol{y} - \hat{\boldsymbol{y}}(\boldsymbol{x})\|_\infty \leq \eta \\ 0, \ else \end{cases}, I_c(\boldsymbol{x}) = \begin{cases} 1, \boldsymbol{C}(\boldsymbol{\theta}, \boldsymbol{x}) \leq \boldsymbol{0} \\ 0, \boldsymbol{C}(\boldsymbol{\theta}, \boldsymbol{x}) > \boldsymbol{0} \end{cases} \tag{6}$$

The following proposition will be used in Section IV for empirical statistical analysis of optimality and feasibility of the trained networks. The proof is followed from the results of Theorem 1 in [16].

Proposition 1: Let $I(\boldsymbol{x})$ be a binary indicator of independently and identically distributed (i.i.d.) random variables $\boldsymbol{x}$ (e.g., indicators given in (6)). Let μ be true mean of $I(\boldsymbol{x})$ and define $\bar{I} = \frac{1}{N}\sum_{i=1}^{N} I(\boldsymbol{x}_i)$ as its empirical mean value estimation by taking samples $\{\boldsymbol{x}_1, \ldots, \boldsymbol{x}_N\}$ over $\boldsymbol{x}$. For small ϵ_h, the following inequality holds.

$$Pr\left[Pr\left(I(\boldsymbol{x}) = 1\right) > \bar{I} - \epsilon_h\right] > \delta_h = 1 - e^{-2N\epsilon_h^2}. \tag{7}$$

where $Pr(\cdot)$ stands for probability of an event.

III. Constrained Deep EMPC

In the proposed learning-based MPC, we consider to only learn $\boldsymbol{u}_k^*$ of (3) at the kth step directly as follows.

$$\hat{\boldsymbol{u}}_k^*(\boldsymbol{x}_k) = \mathcal{N}(\boldsymbol{x}_k; \boldsymbol{\theta}, M, l). \tag{8}$$

Learning $\boldsymbol{u}_k^*$ has two benefits in comparison to learn the whole control sequence $\boldsymbol{U}_k$. First, it would make learning process simplified due to the small-size learning space. Second, constraint learning is simplified as well and this facilitates nonlinear constraint learning. The single step constraint can be summarized as

$$\boldsymbol{C}(\boldsymbol{x}) \leq \boldsymbol{0}. \tag{9}$$

and thus the learning EMPC problem using DNN can be written as

$$\begin{aligned} \min_{\boldsymbol{\theta}}\quad & \mathcal{L}(\boldsymbol{\theta}) = \frac{1}{N} \sum_{i=0}^{N} L\left(\boldsymbol{u}^*(\boldsymbol{x}_i) - \hat{\boldsymbol{u}}^*(\boldsymbol{x}_i)\right) \\ \text{s.t.}\quad & C_j(\boldsymbol{\theta}, \boldsymbol{x}_i) \leq 0,\ j = 1, \ldots, n_c, \end{aligned} \tag{10}$$

where C_j represents the jth element of $\boldsymbol{C}$ in (9). In the above problem (10), we need to deal with $N_s \times n_c$ inequality constraints. Note that inequality constraints cannot be handled with method of Lagrange multiplier in an straightforward manner. Here, we adopt the method introduced in [18] for constraint conversion and constrained network training. In order to do this, note that $C_j(\boldsymbol{\theta}, \boldsymbol{x}) \leq 0$ and $\mathrm{ReLU}\left(C_j(\boldsymbol{\theta}, \boldsymbol{x})\right) = 0$ are equivalent, where $\mathrm{ReLU}(x) = \max(x, 0)$ is applied element-wise. Therefore, we write (10) with equality constraints and furthermore, because of non-negativeness of $\mathrm{ReLU}(\cdot) \geq 0$, $\frac{1}{N}\sum_{i=1}^{N} \mathrm{ReLU}\left(C_j(\boldsymbol{\theta}, \boldsymbol{x}_i)\right) = 0$, is equivalent to $\mathrm{ReLU}\left(C_j(\boldsymbol{\theta}, \boldsymbol{x}_i)\right) = 0$ for any $i = 1, \ldots, N$ and $j = 1, \ldots, n_c$. Thus, the number of constraints is reduced effectively through this process. We summarize the above discussion as

$$\begin{aligned} \min_{\boldsymbol{\theta}} \quad & \mathcal{L}(\boldsymbol{\theta}) = \frac{1}{N}\sum_{i=0}^{N} L\left(\boldsymbol{u}^*(\boldsymbol{x}_i) - \hat{\boldsymbol{u}}^*(\boldsymbol{x}_i)\right) \\ \text{s.t.} \quad & \mathcal{C}_j(\boldsymbol{\theta}) = 0,\ j = 1, \ldots, n_c, \end{aligned} \tag{11}$$

where $\mathcal{C}_j(\boldsymbol{\theta})$, $j = 1, \ldots, n_c$, is defined as

$$\mathcal{C}_j(\boldsymbol{\theta}) = \frac{1}{N}\sum_{i=1}^{N} \mathrm{ReLU}\left(C_j(\boldsymbol{\theta}, \boldsymbol{x}_i)\right). \tag{12}$$

We now introduce Lagrange multiplier matrix $\boldsymbol{\Lambda} = [\lambda_1 \ \cdots \ \lambda_{n_c}]^T$ and convert the constrained minimization of (11) to the following maxmin problem

$$\max_{\boldsymbol{\Lambda}} \min_{\boldsymbol{\theta}} \mathfrak{L}(\boldsymbol{\theta}, \boldsymbol{\Lambda}) = \mathcal{L}(\boldsymbol{\theta}) + \sum_{j=1}^{n_c} \lambda_j \mathcal{C}_j(\boldsymbol{\theta}). \tag{13}$$

The optimization problem of (13) can be solved with a two-step alternating approach, that is, minimization on $\boldsymbol{\theta}$ and maximization on $\boldsymbol{\Lambda}$. We define the following update rules

$$\boldsymbol{\theta}_{t+1} = \boldsymbol{\theta}_t - \alpha_{\boldsymbol{\theta}} \Delta\boldsymbol{\theta}_t(\boldsymbol{\theta}, \boldsymbol{\Lambda}), \tag{14}$$

$$\boldsymbol{\Lambda}_{s+1} = \boldsymbol{\Lambda}_s + \alpha_{\boldsymbol{\Lambda}} \Delta\boldsymbol{\Lambda}_s(\boldsymbol{\theta}, \boldsymbol{\Lambda}), \tag{15}$$

where $t, s \in \mathbb{N}$ are the sequence indexes for $\boldsymbol{\theta}$ and $\boldsymbol{\Lambda}$, respectively. $\alpha_{\boldsymbol{\theta}}$ and $\alpha_{\boldsymbol{\Lambda}}$ are learning rates. The terms $\Delta\boldsymbol{\theta}(\boldsymbol{\theta}, \boldsymbol{\Lambda})$ and $\Delta\boldsymbol{\Lambda}(\boldsymbol{\theta}, \boldsymbol{\Lambda})$ are neural network weight and Lagrange multiplier update increments, respectively. Any gradient based algorithm can be used in (14) and only first-order gradient-based algorithms are implemented in (15). In the current work, L-BFGS and gradient ascent algorithms are used in (14) and (15), respectively. Algorithm 1 illustrates the procedure to train the neural network using the given update rules iteratively. In the algorithm, i_w is number of epochs for initial training of the DNN, d is the outer iteration increment, M is the total number of inner-loop iteration, ϵ is parameter related to outer loop convergence, γ is parameter adjusting Lagrange multiplier learning rate, and $\alpha^0_{\boldsymbol{\Lambda}}$ is initial learning rate for Lagrange multiplier.

Algorithm 1: DNN training and updating procedure

Input : Set: i_w, d, M, ϵ, γ, $\alpha_{\boldsymbol{\theta}}$, and $\alpha^0_{\boldsymbol{\Lambda}}$.
Output:
Initialize: $\boldsymbol{\theta}_0$ randomly, $\boldsymbol{\Lambda}_0 = \mathbf{0}$, $s, t = 0$, $m = 0$;
for i_w **do**
  Update $\boldsymbol{\theta}_t$ using (14) ;
end
while $\|\boldsymbol{\Lambda}_s - \boldsymbol{\Lambda}_{s-1}\|_\infty > \epsilon$ **do**
  Update $\boldsymbol{\Lambda}_s$ using (15) ;
  Increment $s = s + 1$;
  for $m < M$ **do**
    Update $\boldsymbol{\theta}$ using (14) ;
    Increment $t = t + 1$;
  end
  Update $m = m + d$;
  Update learning rate using $\alpha_{\boldsymbol{\Lambda}} = \alpha^0_{\boldsymbol{\Lambda}} \frac{1}{1+\gamma t}$;
end

Stability of the learned policy is an important concern. We now prove that under certain assumptions, the learned approximate policy $\hat{\boldsymbol{u}}^*_k$ stabilizes the dynamic systems.

Assumption 1: Assume that $V(\boldsymbol{x})$ in (2) is a Lyapunov function for the system (1) under MPC (3) with region of attraction $\mathbb{S} \subset \mathbb{R}^n$ and that the following inequalities hold for any $\boldsymbol{x}_k \in \mathbb{S}$

$$V\left(\boldsymbol{x}_{k+1}\right) - V(\boldsymbol{x}_k) \leq -\boldsymbol{x}_k^T \boldsymbol{Q} \boldsymbol{x}_k - {\boldsymbol{u}_k^*}^T \boldsymbol{R} \boldsymbol{u}_k^*. \tag{16}$$

Moreover, $V(\boldsymbol{x})$ is Lipschitz continuous, that is,

$$|V(\boldsymbol{x}) - V(\boldsymbol{y})| \leq \rho \|\boldsymbol{x} - \boldsymbol{y}\|, \tag{17}$$

with $\boldsymbol{x}$, $\boldsymbol{y} \in \mathbb{S}$ and Lipschitz constant $\rho > 0$.

The conditions in Assumption 1 are not restrictive. In fact, it was shown in [20, Theorem 1 and 2] that under mild conditions on the system dynamics, MPC parameters and constraints, Assumption 1 is held. With Assumption 1, the following theorem guarantees stability of the closed-loop system under the learned policy.

Theorem 1: Suppose that Assumption 1 is held and also assume that $\|\boldsymbol{u}_k^* - \hat{\boldsymbol{u}}_k^*\| < \zeta \hat{\boldsymbol{x}}_k^T \boldsymbol{Q} \hat{\boldsymbol{x}}_k$ holds for $\hat{\boldsymbol{x}}_k \in \mathbb{S}$ with $\zeta < \frac{1}{\rho G}$, where $G = \sup_{\boldsymbol{x} \in \mathbb{S}} \|\boldsymbol{g}(\boldsymbol{x})\|$. Then, the closed-loop system of (1) under control $\hat{\boldsymbol{u}}^*_k$ is locally asymptotically stable for $x \in \mathbb{S}$.

Proof: Let us introduce and define $\hat{\boldsymbol{x}}_{k+1} = \boldsymbol{f}(\hat{\boldsymbol{x}}_k) + \boldsymbol{g}(\hat{\boldsymbol{x}}_k)\hat{\boldsymbol{u}}^*_k$. Since time invariant dynamics is considered k is a dummy index [19], thus we can choose $\boldsymbol{x}_k = \hat{\boldsymbol{x}}_k$ in (16). This way, using (17) and $\|\boldsymbol{u}_k^* - \hat{\boldsymbol{u}}_k^*\| < \zeta \hat{\boldsymbol{x}}_k^T \boldsymbol{Q} \hat{\boldsymbol{x}}_k$, we obtain

$$\begin{aligned} |V(\hat{\boldsymbol{x}}_{k+1}) - V(\boldsymbol{x}_{k+1})| &\leq \rho \|\hat{\boldsymbol{x}}_{k+1} - \boldsymbol{x}_{k+1}\| \\ &= \|\boldsymbol{f}(\hat{\boldsymbol{x}}_k) + \boldsymbol{g}(\hat{\boldsymbol{x}}_k)\hat{\boldsymbol{u}}^*_k - \boldsymbol{f}(\hat{\boldsymbol{x}}_k) - \boldsymbol{g}(\hat{\boldsymbol{x}}_k)\boldsymbol{u}^*_k\| \\ &\leq \rho \|\boldsymbol{g}(\hat{\boldsymbol{x}}_k)\| \|\boldsymbol{u}_k^* - \hat{\boldsymbol{u}}_k^*\| \\ &\leq \rho G \|\boldsymbol{u}_k^* - \hat{\boldsymbol{u}}_k^*\| \leq \rho G \zeta \hat{\boldsymbol{x}}_k^T \boldsymbol{Q} \hat{\boldsymbol{x}}_k. \end{aligned}$$

Considering positive definiteness of $V(\boldsymbol{x})$ in the above inequality, we obtain

$$V(\boldsymbol{x}^*_{k+1}) \geq V(\hat{\boldsymbol{x}}^*_{k+1}) - \rho G \zeta \hat{\boldsymbol{x}}_k^T \boldsymbol{Q} \hat{\boldsymbol{x}}_k. \tag{18}$$

Using (18) in (16), and after rearranging, we conclude

$$V(\hat{\boldsymbol{x}}_{k+1}) - V(\hat{\boldsymbol{x}}_k) \leq \left(\rho G \zeta - 1\right) \hat{\boldsymbol{x}}_k^T \boldsymbol{Q} \hat{\boldsymbol{x}}_k. \tag{19}$$

When $\zeta < \frac{1}{\rho G}$, right-hand side of (19) is negative definite for any non-zero $\hat{\boldsymbol{x}}_k \in \mathbb{S}$. Considering this and positive definiteness of $V(\boldsymbol{x})$ per assumption, $V(\boldsymbol{x})$ is a Lyapunov function for

learned control policy $\hat{\boldsymbol{u}}_k^*$ and the closed-loop system is locally asymptotically stable on set $\mathbb{S}$. This completes the proof. ■

IV. Experimental Results

In this section the proposed algorithm is implemented on a rotary inverted pendulum (i.e., Furuta pendulum). Fig. 1 shows the experimental setup (from Quanser Inc.). The Furuta pendulum is commonly used as a benchmark for control algorithms [21]. We use this experimental setup as a benchmark because of its fast dynamic behavior that makes constraint satisfaction challenging. The proposed method is compared with the normally trained DNN that were proposed in [14], [15]. Exact MPC is also used as the base line of comparison in closed-loop control performance. The goal for learning policies is to perform as close as possible to the exact MPC.

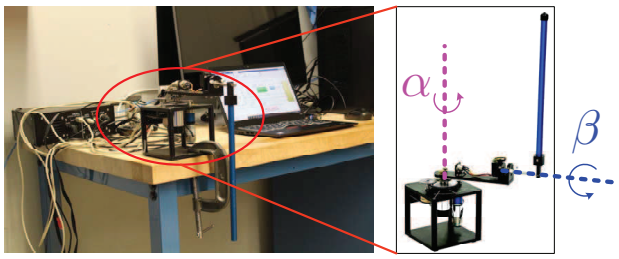

Fig. 1. Rotary inverted pendulum system. The base joint α is actuated and the pendulum joint β is unactuated.

The motion of the Furuta pendulum is captured by an actuated base joint α (powered by a DC motor) and an unactuated pendulum joint β. Using Lagrangian dynamics and the DC motor model, the state space model of the system is obtained as follows.

$$\dot{\boldsymbol{x}} = \boldsymbol{f}_c(\boldsymbol{x}) + \boldsymbol{g}_c(\boldsymbol{x})v, \tag{20}$$

where $\boldsymbol{x} = \begin{bmatrix}\alpha\ \beta\ \dot{\alpha}\ \dot{\beta}\end{bmatrix}^T = [\boldsymbol{q}^T\ \dot{\boldsymbol{q}}^T]^T$, $\boldsymbol{q} = [\alpha\ \beta]^T$, v is the motor voltage, and $\boldsymbol{f}_c(\boldsymbol{x})$ and $\boldsymbol{g}_c(\boldsymbol{x})$ are given as

$$\boldsymbol{f}_c(\boldsymbol{x}) = \begin{bmatrix}\dot{\boldsymbol{q}} \\ \boldsymbol{M}^{-1}(-\boldsymbol{C}\dot{\boldsymbol{q}} - \boldsymbol{G})\end{bmatrix},\ \boldsymbol{g}_c(\boldsymbol{x}) = \begin{bmatrix}\boldsymbol{0}_{2\times 1} \\ \boldsymbol{M}^{-1}\boldsymbol{B}\end{bmatrix},$$

$$\boldsymbol{M} = \begin{bmatrix} m_1 l_1^2 + I_1 + m_2 L_1^2 + m_2 l_2^2\,\mathrm{s}_\beta^2 & m_2 L_1 l_2\,\mathrm{c}_\beta \\ m_2 L_1 l_2\,\mathrm{c}_\beta & m_2 l_2^2 + I_2 \end{bmatrix},$$

$$\boldsymbol{C} = \begin{bmatrix} m_2 l_2^2\,\mathrm{s}_\beta^2\,\dot{\beta} + c_1 + \frac{\eta_m \eta_g K_g^2 K_t K_V}{R_m} & -m_2 L_1 l_2\,\mathrm{s}_\beta\,\dot{\beta} \\ -m_2 l_2^2\,\mathrm{s}_\beta\,\mathrm{c}_\beta\,\dot{\alpha} & c_2 \end{bmatrix}$$

$$\boldsymbol{G} = \begin{bmatrix} 0 \\ -m_2 g l_2\,\mathrm{s}_\beta \end{bmatrix},\ \boldsymbol{B} = \begin{bmatrix} \frac{\eta_m \eta_g K_t K_g}{R_m} \\ 0 \end{bmatrix},$$

where $\mathrm{s}_\beta = \sin\beta$ and $\mathrm{c}_\beta = \cos\beta$ for β and all model parameters are listed in Table I. Euler discretization is used to (20) with sampling time $\Delta T = 0.01$ s to obtain the discrete time model of (1). Online linearization is used to solve nonlinear optimization of (2). MPC parameters are chosen as $\boldsymbol{Q} = \mathrm{diag}\,(8, 3, 0.2, 0.1)$, where diag represents diagonal matrix, $\boldsymbol{R} = 0.1$, and $H = 7$, based on fine tuning on the experimental setup. $\boldsymbol{Q}_f$ is also chosen as the solution of infinite horizon discrete-time Riccati equation for the given $\boldsymbol{Q}$, $\boldsymbol{R}$ and linearized matrices of the system around origin.

TABLE I
System Parameters

Parameter	Description	Nominal values	Unit
m_1	Mass of arm	0.257	Kg
m_2	Mass of pendulum	0.127	Kg
L_1	Length of arm	0.216	m
L_2	Length of pendulum	0.337	m
l_1	CoM of arm	0.0619	m
l_2	CoM of pendulum	0.156	m
I_1	Arm moment of inertia	0.000998	Kgm^2
I_2	Pendulum moment of inertia	0.0012	Kgm^2
c_1	Arm viscous coefficient	0.0024	$\frac{\text{N.m}}{\text{rad/s}}$
c_2	Pendulum viscous coefficient	0.0024	$\frac{\text{N.m}}{\text{rad/s}}$
K_g	Gearbox ratio	70	-
K_t	Motor torque constant	0.00768	$\frac{\text{N.m}}{\text{A}}$
K_V	Motor back-emf constant	0.00768	$\frac{\text{N.m}}{\text{rad/s}}$
R_m	Motor winding resistance	2.6	Ohm
η_m	Motor efficiency	0.69	-
η_g	Gearbox efficiency	0.9	-

The MPC constraints are $|v| \leq 6$, $|\alpha| \leq \pi/3$, $|\dot{\alpha}| \leq 6$, and $|\dot{\beta}| \leq 15$.

A. Constrained Learning MPC

A deep MLP, with $g(x) = \tanh(x)$ activation function in hidden units, is used. The network has $l = 8$ layers with $M = 30$ nodes in each hidden layer as in (4). By this configuration, the network has $5,760$ learnable parameters.

1) Data sampling: Appropriate data for training is a crucial part of learning algorithms [7]. Often, two techniques are used in literature for sampling data for learning MPC policies including uniform sampling (e.g., [11]) and data from random trajectories (e.g., [10]). Despite vast research on learning MPC it is not clear which sampling technique provides better generalization error. Here, different data sampling techniques are assessed based on generalization error of learned policies (of normally trained network) on data sets of size $100,000$ from different sampling techniques. Five sampling techniques are considered as follows, where exact MPC is used to generate the data sets.

- S1. Trajectories with random initial states and fixed length enough for convergence of the trajectory.
- S2. Trajectories with random initial states and lengths.
- S3. Random uniform sampling.
- S4. Random uniform sampling by dividing the data set to 20% with active control constraint and %80 without active control constraint.
- S5. Uniform combination of 1-4 by combining data from 1-4 (25% from each sampling technique).

We used the above five sampling techniques to separately train and obtain DNNs. Then, we calculated generalization error statistics of each neural network on five different test sets obtained through S1-S5. The standard deviation of errors are summarized in Table II. As shown in the table, the best generalization error is for the neural network trained with combination data set, that is S5. It is also noted that dividing uniform sampled data to those with active and inactive control

TABLE II

STD OF LEARNED POLICY ERROR FOR DIFFERENT SAMPLING METHODS

Train set	Test set				
	S1	S2	S3	S4	S5
S1	3.3%	11%	49%	57%	38%
S2	3.3%	4.5%	28%	32%	22%
S3	15%	17%	7%	12%	13%
S4	10%	11%	7%	9%	9%
S5	4.5%	6%	8%	12%	8%

TABLE III

EMPIRICAL STATISTICS OF LEARNED POLICIES

Parameter		Normal training	Constrained training
Optimality error	Mean	0.0%	0.0%
	STD	3.3%	3.6%
State Constraint violation		3.14%	0.86%
Control Constraint violation		6.53%	0.07%
Total Constraint violation		9.67%	0.93%

constraints effectively decreases generalization error. This is because with uniform sampling majority of the data has active control constraints. It is therefore desirable to use uniform sampling technique for systems with tight control constraints. In this study, it is of interest in prediction over converged trajectories and the second data sampling technique S2 is chosen for the following implementation since it provides lowest prediction error over converged trajectories data set.

2) Learning procedure: To train both networks, $100,000$-point and $10,000$-point data sets are collected from trajectories with random initial states and lengths for training and testing, respectively. We used PyTorch™ for neural network training. For normally trained network, L-BFGS method is used for $2,000$ epochs after which error plateaus. To train constrained network, Algorithm 1 is implemented. A warm-up training with $1,200$ epochs was conducted using L-BFGS method. This is followed by 700 epochs of constraint training with combination of L-BFGS and gradient ascent methods. The training completes with 100 epochs of fine tuning. In this way total epoch for training both neural networks are the same.

3) Statistical analysis of learned policies: Empirical analysis of optimality and constraint satisfaction of the trained policies is done on $100,000$ data set. Table III summarizes the comparison results between the normal and the proposed training approaches. It is clear that the proposed training significantly outperforms the normal training process in various criteria as shown in the table.

Empirical confidence levels are calculated using proposition 1. Choosing $\eta = 0.3$, representing five percent of maximum voltage, and $\epsilon_h = 0.01$, we have $\delta_h \simeq 0.99$. $\bar{I}_o(\boldsymbol{x}) = 98.8\%$ and $\bar{I}_c(\boldsymbol{x}) = 90.3\%$ are achieved for the normally trained network. Using these in proposition 1, we obtain following probabilities with 99% confidence level

$$Pr\left(I_o(\boldsymbol{x}) = 1\right) > 0.978,\ Pr\left(I_c(\boldsymbol{x}) = 1\right) > 0.893.$$

Similarly, $\bar{I}_o(\boldsymbol{x}) = 98.6\%$ and $\bar{I}_c(\boldsymbol{x}) = 99.1\%$ are achieved for proposed constraint trained network. Using these values in Proposition 1, we obtain the following statements with 99% confidence levels

$$Pr\left(I_o(\boldsymbol{x}) = 1\right) > 0.976,\ Pr\left(I_c(\boldsymbol{x}) = 1\right) > 0.981,$$

It is clear that using constrained learning algorithm increases constraint satisfaction guarantees while maintains the suboptimality achieved by normal training.

Deep learning based MPC has already been proved to be dramatically more computationally efficient than exact MPC even for simple problems [8], [11], [13]. The final structure of the constrained network is the same as the normally trained network and thus, they have same online computational cost. We calculated the average computational time using Matlab™ functions on a personal Core i5™ laptop with 4 GB RAM. The exact MPC takes on average 5 ms, while the deep learning based MPC takes on average 0.1 ms. This estimation indicates the deep learning-based controller approximately achieves 50 times faster than the normal training MPC. This result is compatible with that presented in [8].

B. Experimental Results

Control performance of the proposed method is compared with normally trained deep MPC and exact MPC using rotary inverted pendulum experiments. In the test, the pendulum's initial condition is considered as $\boldsymbol{x}_0 = [\pi/3\,0\,0\,0]^T$. Fig. 2 shows the joint angle and angular velocity profiles under these three control designs while Fig. 3 illustrates the corresponding control inputs.

From Fig. 2, the trajectories under the both normally and the constrained trained networks perform closely to that under the exact MPC in most time. However, the learned policies face a challenge replicating exact MPC behavior when the arm's angular velocity constraints are saturated while pendulum is near equilibrium point as shown in the zoom-in plots. This happens at around $t = 1.6$ s; see Fig. 2(a) and the constrained network continues to perform closely to that under the exact MPC, but the normally trained network has a shift in its response after satisfying the constraint. This is due to conflicting nature of the two tasks, namely, satisfying the arm angular velocity constraint and keeping pendulum upright. It can also be seen in Figs. 2 and 3 that after around $t = 2$ s both the learned policies have slightly different behavior than the exact MPC. This is due to the fact that in the close vicinity of equilibrium point, the stick-slip frictional phenomenon is dominant in the system [22]. In term of optimality comparison, the normally trained networks controller achieves 4.6% suboptimal in comparison to exact MPC, while the constrained trained controller is 2.4% and again, the latter outperforms the former design.

V. CONCLUSION

In this work, we proposed a constrained deep neural networks-based MPC. The constrained neural network training approach improved constraints satisfaction while did not change sub-optimality and efficacy of the learned policy. Lyapunov stability of the learned policy was also analyzed to show the convergence under the learned MPC strategy. Different sampling techniques were also examined to demonstrate

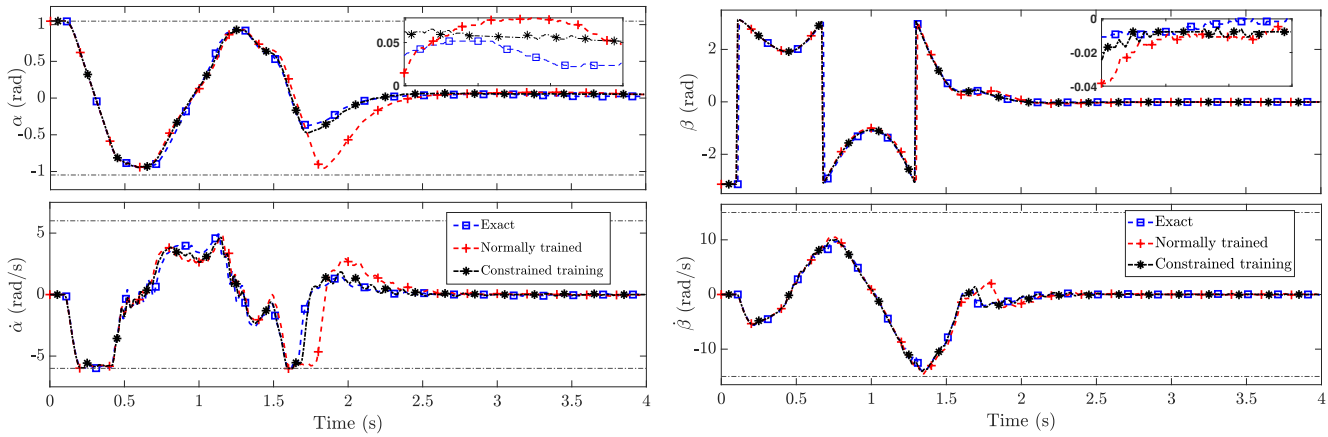

Fig. 2. Experimental and comparison results. (a) Base angle α and angular velocity $\dot{\alpha}$. (b) Pendulum angle β and angular velocity $\dot{\beta}$.

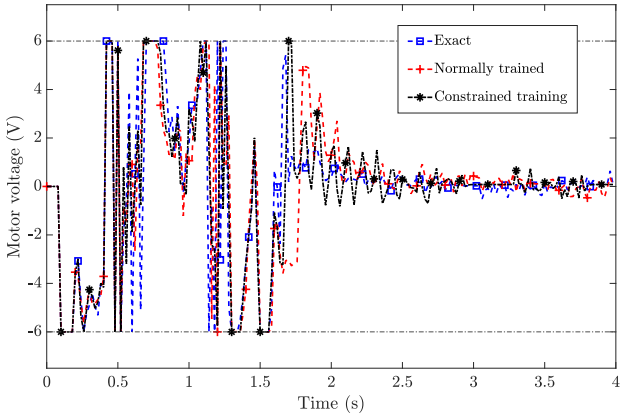

Fig. 3. The motor voltage under various controllers.

the DNN training performance. Experimental implementation was conducted on rotary inverted pendulum to validate and demonstrate the proposed constrained MPC. The experimental comparison with two other MPC controllers demonstrated the superior performance of the proposed design.

REFERENCES

[1] J. B. Rawlings, D. Q. Mayne, and M. Diehl, *Model predictive control: theory, computation, and design*. Nob Hill Publishing Madison, WI, 2017, vol. 2.

[2] A. Zanelli, A. Domahidi, J. Jerez, and M. Morari, "Forces nlp: an efficient implementation of interior-point methods for multistage nonlinear nonconvex programs," *Int. J. Control*, vol. 93, no. 1, pp. 13–29, 2020.

[3] S. Lucia, D. Navarro, Ó. Lucía, P. Zometa, and R. Findeisen, "Optimized fpga implementation of model predictive control for embedded systems using high-level synthesis tool," *IEEE Trans. Ind. Informat.*, vol. 14, no. 1, pp. 137–145, 2017.

[4] J. Drgona, K. Kis, A. Tuor, D. Vrabie, and M. Klauco, "Differentiable predictive control: An mpc alternative for unknown nonlinear systems using constrained deep learning," *arXiv preprint arXiv:2011.03699*, 2020.

[5] F. Borrelli, A. Bemporad, and M. Morari, *Predictive control for linear and hybrid systems*. Cambridge University Press, 2017.

[6] A. Gersnoviez, M. Brox, and I. Baturone, "High-speed and low-cost implementation of explicit model predictive controllers," *IEEE Trans. Contr. Syst. Technol.*, vol. 27, no. 2, pp. 647–662, 2017.

[7] I. Goodfellow, Y. Bengio, and A. Courville, *Deep Learning*. MIT Press, 2016, http://www.deeplearningbook.org.

[8] X. Zhang, M. Bujarbaruah, and F. Borrelli, "Near-optimal rapid mpc using neural networks: A primal-dual policy learning framework," *IEEE Trans. Contr. Syst. Technol.*, 2021, in press.

[9] S. Chen, K. Saulnier, N. Atanasov, D. D. Lee, V. Kumar, G. J. Pappas, and M. Morari, "Approximating explicit model predictive control using constrained neural networks," in *Proc. Amer. Control Conf.*, 2018, pp. 1520–1527.

[10] B. Karg and S. Lucia, "Efficient representation and approximation of model predictive control laws via deep learning," *IEEE Trans. Cybernetics*, vol. 50, no. 9, pp. 3866–3878, 2020.

[11] E. T. Maddalena, C. d. S. Moraes, G. Waltrich, and C. N. Jones, "A neural network architecture to learn explicit mpc controllers from data," *arXiv preprint arXiv:1911.10789*, 2019.

[12] J. Ferlez and Y. Shoukry, "Aren: assured relu nn architecture for model predictive control of lti systems," in *Proc. Int. Conf. Hybrid Systems: Computation and Control*, 2020, pp. 1–11.

[13] M. Hertneck, J. Köhler, S. Trimpe, and F. Allgöwer, "Learning an approximate model predictive controller with guarantees," *IEEE Control Syst. Lett.*, vol. 2, no. 3, pp. 543–548, 2018.

[14] S. Lucia and B. Karg, "A deep learning-based approach to robust nonlinear model predictive control," *IFAC-PaperOnLine*, vol. 51, no. 20, pp. 511–516, 2018.

[15] J. Nubert, J. Köhler, V. Berenz, F. Allgöwer, and S. Trimpe, "Safe and fast tracking on a robot manipulator: Robust mpc and neural network control," *IEEE Robot. Automat. Lett.*, vol. 5, no. 2, pp. 3050–3057, 2020.

[16] W. Hoeffding, "Probability inequalities for sums of bounded random variables," in *The Collected Works of Wassily Hoeffding*. Springer, 1994, pp. 409–426.

[17] P. Márquez-Neila, M. Salzmann, and P. Fua, "Imposing hard constraints on deep networks: Promises and limitations," *arXiv preprint arXiv:1706.02025*, 2017.

[18] Y. Nandwani, A. Pathak, P. Singla *et al.*, "A primal dual formulation for deep learning with constraints," in *Advances in Neural Information Processing Systems*. NeurIPS, 2019, pp. 12 157–12 168.

[19] D. Q. Mayne, J. B. Rawlings, C. V. Rao, and P. O. Scokaert, "Constrained model predictive control: Stability and optimality," *Automatica*, vol. 36, no. 6, pp. 789–814, 2000.

[20] G. De Nicolao, L. Magni, and R. Scattolini, "Stabilizing receding-horizon control of nonlinear time-varying systems," *IEEE Trans. Automatic Control*, vol. 43, no. 7, pp. 1030–1036, 1998.

[21] F. Han and J. Yi, "Stable learning-based tracking control of underactuated balance robots," *IEEE Robot. Automat. Lett.*, vol. 6, no. 2, pp. 1543–1550, 2021.

[22] G. Albertini, S. Karrer, M. D. Grigoriu, and D. S. Kammer, "Stochastic properties of static friction," *J. Mech. Phy. Solids*, vol. 147, pp. 1–17, 2021.

This figure "furuta_dev.jpg" is available in "jpg" format from:

http://arxiv.org/ps/2103.13514v1